2014

New Invariant Measures to Track Slow Parameter Drifts in Fast Dynamical Systems

Son Hai Nguyen
University of Rhode Island

David Chelidze
University of Rhode Island, chelidze@uri.edu

Citation/Publisher Attribution
Son Hai Nguyen and David Chelidze. (2014). New invariant measures to track slow parameter drifts in fast dynamical systems. Nonlinear Dynamics, 79(2), 1207-1216. doi: 10.1007/s11071-014-1737-y
Available at: http://dx.doi.org/10.1007/s11071-014-1737-y

Nonlinear Dynamics manuscript No.
(will be inserted by the editor)

New invariant measures to track slow parameter drifts in fast dynamical systems

Son Hai Nguyen · David Chelidze

Received: date / Accepted: date

Abstract Estimates of quantitative characteristics of nonlinear dynamics, e.g., correlation dimension or Lyapunov exponents, require long time series and are sensitive to noise. Other measures (e.g., phase space warping or sensitivity vector fields) are relatively difficult to implement and computationally intensive. In this paper, we propose a new class of features based on Birkhoff Ergodic Theorem, which are fast and easy to calculate. They are robust to noise and do not require large data or computational resources. Application of these metrics in conjunction with the smooth orthogonal decomposition to identify/track slowly changing parameters in nonlinear dynamical systems is demonstrated using both synthetic and experimental data.

Keywords dynamical systems · invariant measures · characteristic distance · smooth orthogonal decomposition · parameter tracking

1 Introduction

Classifying and identifying nonlinear dynamical systems are some of basic tasks in nonlinear time-series analysis [1,9,14]. Most generic approach is to rely on some feature metric that is invariant under the evolution of the dynamics. Conventional methods often characterize a dynamical system using long-time invariant quantities such as Lyapunov exponents or fractal dimensions [13,12,16,10]. Fractal dimensions provide bounds on the number of active degrees-of-freedom and reflect the complexity of the system. Lyapunov exponents characterize the average exponential divergence rates of infinitesimally close trajectories on the attractor, and are used to infer if the underlying system is integrable or chaotic.

Application of these metrics in vibrations-based structural health monitoring has been studied extensively [18, 19,11]. However, reliable estimation of Lyapunov exponents from the observed time series is difficult in the presence of noise, complicated by the fact that they are not exactly defined for noisy data [20]. Literature survey of techniques developed for the computation of Lyapunov exponents is extensive [2]. Most of the methods monitor the evolution of system dynamics for thousands of time steps. Therefore, large experimental data requirements and extensive computation time impose limits on their practical applications. To deal with these problems, Clement and Laurens proposed the Jacobian Feature Vector [7] which is based on Lyapunov exponent's algorithm but has faster computation. Other interesting feature extracted from measured data has been studied by Todd *et al.* [17], where local attractor variance ratio is described as a change in geometric properties of an attractor.

All these quantities describe the long-time behavior of a dynamical system. Although they are able to detect sudden changes in a system, they are ill-suited for continuous tracking of slowly changing parameters responsible for nonstationarity in a dynamical systems. In previous work [3,4], a concept of *phase space warping* (PSW) was proposed to characterize changes in slow parameter drifts in the fast-time flow. A one-to-one relationship between PSW-based tracking vectors and actual slow-time variables causing these changes has been demonstrated. However, this procedure requires considerable computational time and resources for estimation.

Department of Mechanical, Industrial and Systems Engineering, University of Rhode Island, Kingston, RI 02881, USA
Tel.: +1.401.874.2356, Fax: +1.401.874.2355
E-mail: chelidze@egr.uri.edu

In many practical application like in MEMS-based sensors (e.g., in atomic force microscopy), observed data is accumulated at such high rates that it is impractical to record the raw time series or do complicated online analysis. Hence, it is more practical to do simple, easy to calculate feature extraction locally on the sensor and only output feature time series at much lower sampling rates. However, local processing has limited storage and computational resources, and it requires fairly simple and easy to estimate features (most use mean, variance, or resonant frequency estimations). These simple features do not capture important nonlinear behaviors and have limited application scope. To address this problem, a new class of simple nonlinear features that are fast to calculate and do not require large data are presented here. These metrics are applicable in situations where fast online computation is needed.

In the next section, new metrics called characteristic distance and position are introduced. The existence, uniqueness and invariance properties are demonstrated using Birkhoff Ergodic Theorem [21]. These metrics can be seen as nonlinear statistical quantities characterizing a deterministic dynamical system. Then a new method to track slowly varying parameters using characteristic distances is presented and is verified by both synthetic and experimental data. This is followed by the discussion of results and conclusions.

2 A New Class of Nonlinear Metrics

Lyapunov exponents and fractal dimensions are rooted in Ergodic theory [21] which is originally developed to identify and classify invariant measures under the time evolution. In the following, one of the important theorems in Ergodic theory, Birkhoff Ergodic Theorem, is restated for completeness. Then a new class of characteristics of nonlinear dynamics based on this theorem is proposed.

2.1 Birkhoff Ergodic Theorem

Consider the time evolution of a dynamical system, measured in discrete time units, given by a transformation $\mathcal{T} : X \to X$, so that if $\mathbf{x} \in X \subset \mathbb{R}^n$ is the current state then $\mathcal{T}(\mathbf{x})$ is the state of the system after one time unit. If the system is at the steady state, by the invariant property $\mathcal{T}(X) \subseteq X$ then $\mathcal{T}$ is a measure preserving transformation. For example, let X be the phase space of a mechanical system. Then every point of X represents the values of position and momentum variables. A measurement of the system (e.g., velocity, acceleration) can be defined by a function $f : X \to \mathbb{R}$. To measure a quantity of the system, one usually takes n successive measurements $f(\mathbf{x}), f\left(\mathcal{T}(\mathbf{x})\right), \ldots, f\left(\mathcal{T}^n(\mathbf{x})\right)$ and looks at their average. The question is if the average exists and is invariant when $n \to \infty$. Ergodic theory is originally developed to answer this question.

Birkhoff Ergodic Theorem for measure preserving transformation [21]: Let (X, B, μ) be a finite measure space. Let $\mathcal{T} : X \to X$ be a measure preserving transformation. For any $f \in L^1(X, B, \mu)$ the following limit

$$\lim_{n\to\infty} \frac{1}{n} \sum_{k=0}^{n-1} f\left(\mathcal{T}^k(\mathbf{x})\right) \tag{1}$$

exists and is invariant.

Using this theorem, we can define useful invariant metrics for a dynamical system's attractor which are fast, easy to calculate, robust to noise, and do not require large data or computational resources.

2.2 Characteristic Distance and Position

Let $f : X \to \mathbb{R}$ be a measurable function, which is the Euclidean distance between a point $\mathbf{x} \in X$ and some fixed point $\mathbf{y} \in R^n$,

$$f(\mathbf{x}) = \|\mathbf{x} - \mathbf{y}\|_2 \,. \tag{2}$$

Then a scalar *characteristic distance* $D(\mathbf{y})$ can be defined as a limit

$$D(\mathbf{y}) = \lim_{n\to\infty} \frac{1}{n} \sum_{i=0}^{n-1} f(\mathcal{T}^i(\mathbf{x}))\,. \tag{3}$$

By the Birkhoff Ergodic Theorem, the characteristic distance is an invariant measure on an attractor. It can be seen as an average distance from an arbitrary fixed point in the phase space to an attractor.

There is nothing particularly special about this characteristic distance metric other than it is easy to define and estimate. Other similar metrics can also be defined and may be more appropriate in different applications. For example, we will also define and use vector-valued *characteristic position* as

$$\mathbf{P}(\mathbf{y}) = \lim_{n\to\infty} \frac{1}{n} \sum_{i=0}^{n-1} \mathbf{f}_p(\mathcal{T}^i(\mathbf{x}))\,, \tag{4}$$

where again $\mathbf{y} \in \mathbb{R}^n$, and $\mathbf{f}_p : X \to \mathbb{R}^n$ is defined as

$$\mathbf{f}_p(\mathbf{x}) = \frac{\mathbf{x} - \mathbf{y}}{\|\mathbf{x} - \mathbf{y}\|_2}\,. \tag{5}$$

3 Reconstructing Slowly Drifting Variables

We consider a coupled dynamical system where a slow-time state variable causes drifts in the parameters of a fast-time subsystem:

$$\dot{\mathbf{x}} = \mathbf{f}(\mathbf{x}, \boldsymbol{\mu}(\boldsymbol{\phi}), t), \quad \dot{\boldsymbol{\phi}} = \epsilon \mathbf{g}(\boldsymbol{\phi}, t), \tag{6}$$

where $\mathbf{x} \in X \subset \mathbb{R}^n$ is a fast-time dynamic variable, $\boldsymbol{\phi} \in P \subset \mathbb{R}^m$ is a hidden slow-time dynamic variable, which alters the parameter vector $\boldsymbol{\mu} \in \mathbb{R}^p$. $t \in \mathbb{T} \subset \mathbb{R}$ is time, overdots denote time differentiation, $0 < \epsilon \ll 1$ is a small rate constant defining the time scale separation. This formulation is relevant to tracking and identifying damage processes as discussed in [5]. It is assumed that the variable $\boldsymbol{\phi}$ changes slowly. Thus, $\boldsymbol{\phi}$ is considered as approximately constant for a fast-time data set collected over an intermediate time interval.

A general solution to the fast subsystem of Eq. (6) can be written as $\mathbf{x} = \mathbf{X}(t, \mathbf{x}_0, \boldsymbol{\phi})$, where $\mathbf{x}_0$ is the initial condition. Hence, the continuous form of the characteristic distance for a fixed point $\mathbf{y}$ can be expressed as

$$D(\mathbf{y}) = \lim_{T\to\infty} \frac{1}{T} \int_0^T \|\mathbf{y} - \mathbf{X}(t, \mathbf{x}_0, \boldsymbol{\phi})\|_2 \, dt \,. \tag{7}$$

This limit is approximated by the integral

$$D(\mathbf{y}) \approx \frac{1}{T_n} \int_0^{T_n} \|\mathbf{y} - \mathbf{X}(t, \mathbf{x}_0, \boldsymbol{\phi})\|_2 \, dt \,, \tag{8}$$

where T_n is a large number. By the Mean Value Theorem for integrals, there is a $t_i \in [0, T_n]$ such that

$$\frac{1}{T_n} \int_0^{T_n} \|\mathbf{y} - \mathbf{X}(t, \mathbf{x}_0, \boldsymbol{\phi})\|_2 \, dt = \|\mathbf{y} - \mathbf{X}(t_i, \mathbf{x}_0, \boldsymbol{\phi})\|_2 \,. \tag{9}$$

Therefore, an estimated value of $D(\mathbf{y})$ is a direct function of $\boldsymbol{\phi}$.[1] Because of bifurcations, the position of the attractor may change dramatically, therefore the characteristic distance $D(\mathbf{y})$ is not expected to be a continuous function of $\boldsymbol{\phi}$. However, the estimated characteristic distances may still provide valuable information about the parameter drifts in the system. In what follows, $D(\mathbf{y})$ for different points $\mathbf{y}$ will be used to reconstruct slow state variable $\boldsymbol{\phi}$.

It is assumed that scalar time series measured from a fast-time subsystem are recorded into m consecutive data sets. Each of the ith data set ($i = 1, \ldots, m$) is recorded over the intermediate time interval over which the variations in the slow variable are assumed negligible $\boldsymbol{\phi} \approx \boldsymbol{\phi}_i = \langle \boldsymbol{\phi} \rangle_i$, where $\langle \boldsymbol{\phi} \rangle_i$ is the average value of $\boldsymbol{\phi}$ within the ith data set. However, $\boldsymbol{\phi}_i$ itself changes gradually from one data set to another.

The characteristic distances are calculated for each data set and are assembled together in a feature vector

$$\mathbf{Y}^i = [D(\boldsymbol{\phi}_i, \mathbf{y}_1); D(\boldsymbol{\phi}_i, \mathbf{y}_2); \ldots; D(\boldsymbol{\phi}_i, \mathbf{y}_n)] \,, \tag{10}$$

where $\{\mathbf{y}_i\}_{i=1}^n$ are randomly chosen fixed points in the phase space. These feature vectors describe the gradual evolution of slow state variable $\boldsymbol{\phi}$ and are concatenated in time sequence into tracking matrix $\mathbf{Y} \in \mathbb{R}^{m\times n}$ in time sequence. This matrix $\mathbf{Y}$ embeds the changes in the parameters of the fast-time subsystem.

Previously, *smooth orthogonal decomposition* SOD [4, 6] has been used for identifying smooth trends in multivariate time series. Here, we also use SOD to extract deterministic slow trends from $\mathbf{Y}$. SOD analysis is performed using generalized singular value decomposition of matrix $\mathbf{Y}$ and its time derivative $\mathbf{DY}$, where $\mathbf{D}$ is a discrete differential operator. These matrices are decomposed as:

$$\mathbf{Y} = \mathbf{UCX}^T \quad \text{and} \quad \mathbf{DY} = \mathbf{VSX}^T \,, \tag{11}$$

where $\mathbf{U}$ and $\mathbf{V}$ are unitary matrices, $\mathbf{C}$ and $\mathbf{S}$ are diagonal matrices, and $\mathbf{X}$ is a square matrix. The *smooth orthogonal coordinates* (SOCs) are given by the columns of $\mathbf{UC}$, *smooth projective modes* (SPMs) are provided by columns of $\mathbf{X}^{-T}$, and *smooth orthogonal values* (SOVs) are $\boldsymbol{\sigma} = \mathrm{diag}(\mathbf{C}^T\mathbf{C})./\mathrm{diag}(\mathbf{S}^T\mathbf{S})$ ('./' indicates term by term division). The greater the magnitude of the SOV the smoother in time is its corresponding SOC. Since the slow-time state variable is a product of a smooth deterministic process, we hypothesis that this variable is embedded in the smoothest SOCs.

4 Numerical Validation

In the following, the time series derived from a Rössler and a Duffing equations are used to validate our slow variable tracking algorithm. In the simulations, a slow-time variable is introduced by slowly varying a parameter in the equations.

Rössler Equation is given by

$$\begin{aligned} \dot{x} &= -y - z \,, \\ \dot{y} &= x + ay \,, \\ \dot{z} &= b + z(x - c) \,. \end{aligned} \tag{12}$$

In our simulations, b is fixed at 0.6, c is fixed at 6.0, and a is varied sinusoidally from 0.1 to 0.4. Here, a is considered a slow-time variable. For each particular value of a, 100,000 steady state trajectory points are generated with time step $t_s = 0.06$. The bifurcation

[1] The same derivation can also be repeated for the characteristic position metric to show that $\mathbf{P}(\mathbf{y})$ is also a direct function of $\boldsymbol{\phi}$.

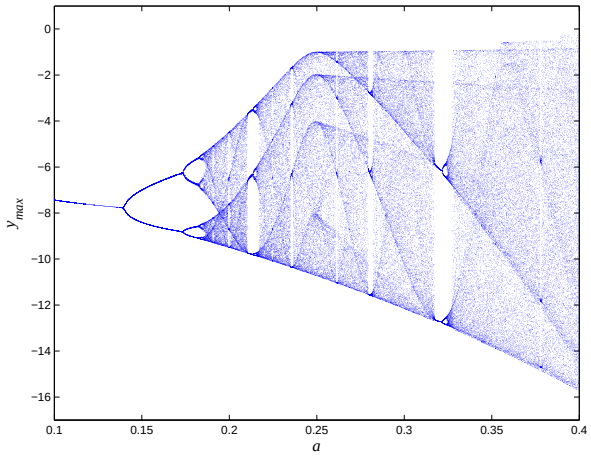

Fig. 1: Bifurcation diagram for Rössler equation

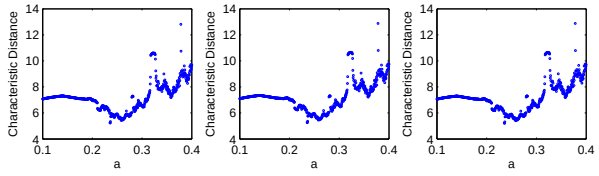

Fig. 2: The characteristic distances versus a for three randomly chosen fixed points in the phase space

diagram is shown in Fig. 1. Filled-in regions of the plot indicate chaotic regions.

Then characteristic distances from 50 arbitrarily chosen fixed points are estimated. Fig. 2 shows the plot of characteristic distance as a function of the bifurcation parameter a. Finally, the 786×50 tracking matrix $\mathbf{Y}$ is assembled. The tracking results after applying SOD to this matrix are shown in Fig. 3. Fig. 3(a) shows the first SOV is much larger than the rest, which is consistent with the fact that there is only one slowly varying parameter in the system. The SOC corresponding to the largest SOV is depicted in Fig. 3(c). To indicate the strength of the linear relationship between the real slow state variable, as shown in Fig. 3(b), and the first SOC, the correlation coefficient r is calculated. $r \approx 1$ shows that there is a strong linear relationship between the two variables as seen in Fig. 3(d).

Duffing Equation In the previous example, the real phase space of Rössler equation is used to calculate the characteristic distances. In this example, only a time series x from a two-well Duffing equation is considered:

$$\ddot{x} + \gamma\dot{x} + \alpha x + \beta x^3 = f\cos\omega t \tag{13}$$

where the system's parameters and forcing frequency are fixed to $\gamma = .25$, $\alpha = -1$, $\beta = 1$, and $\omega = 1$. f is used

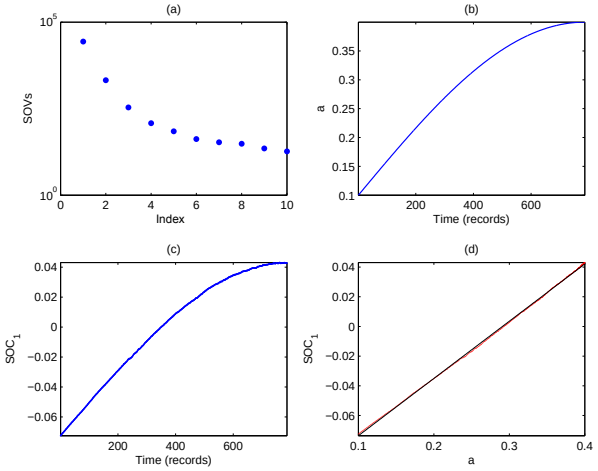

Fig. 3: First ten SOVs (a), parameter a versus time (b), dominant SOC_1 corresponding to the largest SOV (c), plot of SOC_1 versus parameter a (red dots) with least square linear fit (black line) (d). The correlation coefficient between a and SOC_1 is $r = 0.9999$.

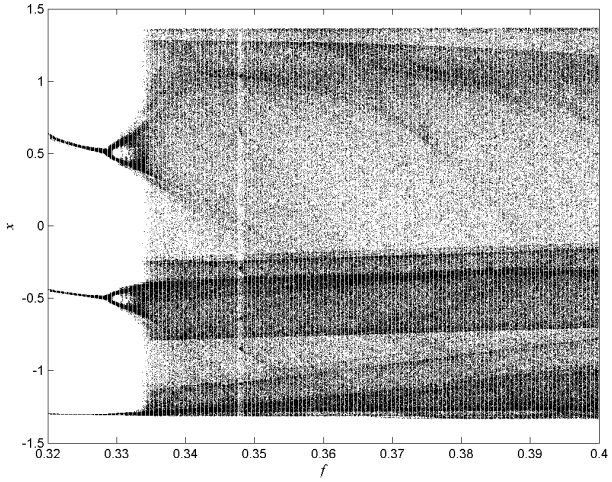

Fig. 4: Bifurcation diagram for Duffing oscillator

as a slowly drifting variable or a bifurcation parameter. The bifurcation diagram is shown in the Fig. 4. We consider the case when f is changed slowly and linearly from 0.35 to 0.4. In this range of f, the response of the system is in the chaotic region.

In the calculations, the first 50 cycles of data are dropped, and 100,000 steady state points are recorded for each forcing amplitude using a sampling time $t = \pi/36$. The phase space is then reconstructed using a time delay $\tau = 53$ and embedding dimension $d = 4$ [14, 1]. Fig. 5 shows the characteristic distances to the reconstructed phase space from three randomly chosen points.

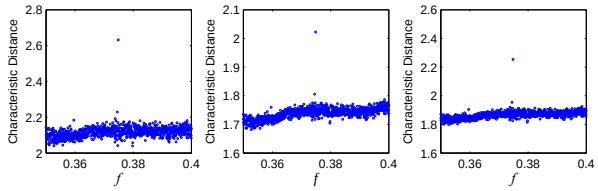

Fig. 5: Characteristic distances from the three randomly chosen points in the phase space of the Duffing oscillator

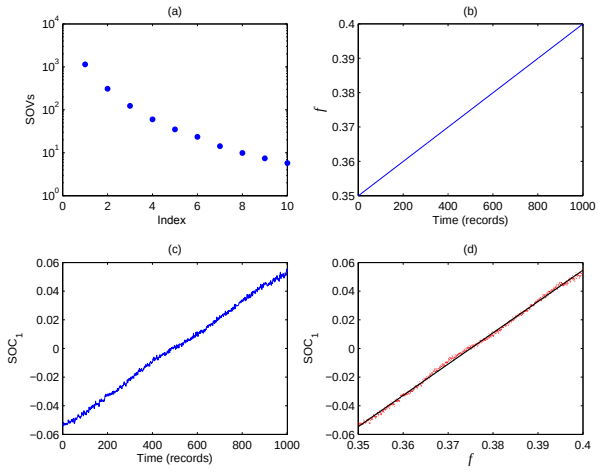

Fig. 6: First ten SOVs (a), parameter f versus time (b), dominant SOC_1 corresponding to the largest SOV (c), plot of SOC_1 versus parameter f (red dots) with least square linear fit (black line) (d). The correlation coefficient between f and SOC_1 is $r = 0.9991$.

400 randomly chosen points in the phase space are used to assemble 1001×400 tracking matrix $\mathbf{Y}$. Then the SOD-based tracking result is shown in Fig. 6. Again, we obtain a linear relationship between the smoothest SOC_1 and the real slowly drifting variable f as seen in Fig. 6(d). Please note that these tracking results are still possible even when each component of matrix $\mathbf{Y}$ is discontinuous as shown in Figs. 2 and 5.

5 Experimental Validation

Data generated from a modified version [8] of the well known two-well magneto-elastic oscillator [15] is used to validate this new approach to slow-parameter tracking. Description of this experiment is given in Ref. [6]. The basic schematic of the experiment is shown in Fig. 7. In this experiment, a couple of electromagnets powered by a computer-controlled power supply are used to cause perturbations in the magnetic potential at the free end

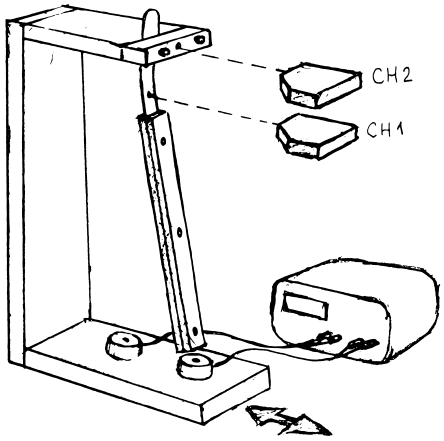

Fig. 7: Schematic of the experimental apparatus

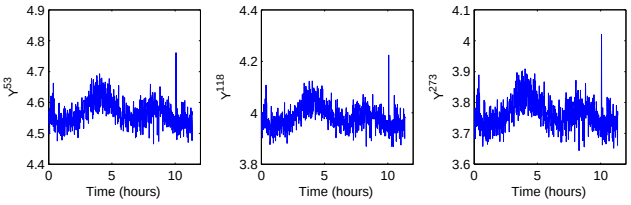

Fig. 8: Three randomly chosen column of the tracking matrix

of a vibrating cantilever beam. The vibration of the beam is measured by two laser vibrometers (CH1, CH2) mounted near the clamped end of the stiffened beam. The position of the beam is calculated by the difference between CH1 and CH2. The beam is excited by a 10 Hz harmonic load, and its amplitude is set so the beam undergoes nominally chaotic cross-well oscillations for fully loaded (10 V) electromagnets. Vibration data is low-pass filtered with 50 Hz cut off frequency and collected at a 160 Hz sampling frequency.

The voltages supplied to the electromagnets ($v_1(t)$ and $v_2(t)$) are altered harmonically and independently as shown in Fig. 9(b). These voltages play a role of slow state variables in the system.

The experiment lasts about 12 hours and 6.6 million data points are recorded [6]. The 5-dimensional fast-time phase space is reconstructed using a delay time of six time samples ($t_s = 1/160$ s). The time series are split into 800 data records, and each record contains 2^{13} points. Here, the characteristic distances are calculated from 300 fixed points randomly chosen in the reconstructed phase space. Then the 800×300 tracking matrix $\mathbf{Y}$ is assembled. Three randomly chosen columns of the tracking matrix are shown in Fig. 8.

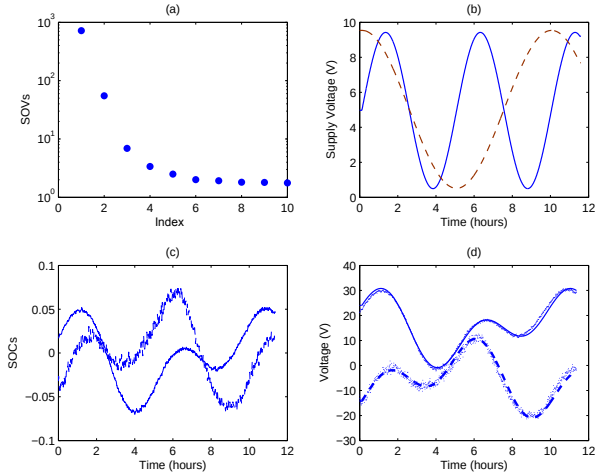

Fig. 9: Plot of ten largest SOVs (a); actual electromagnet supply voltages v_1 (—) & v_2 (- -) versus time plot (b); plot of the first (—) and second (- -) SOCs corresponding to the two largest SOVs (c); plots of $v_1 + v_2$ (—), $v_1 - v_2$ (- -), and the scaled first two SOCs (.) (d).

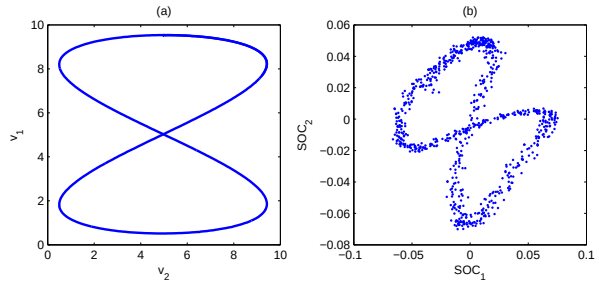

Fig. 10: Phase portrait of the power supply terminal voltages (a) and two smoothest SOCs (b)

The SOD-based tracking result is shown in Fig. 9(a) and (c). The two largest SOVs are several orders-of-magnitude larger than the rest, which is consistent with two-dimensional slowly varying variable in the system. The SOCs corresponding to these two largest SOVs are depicted in Fig. 9(c). The phase portraits of the actual power supply terminal voltages and two smoothest SOCs are shown in Fig. 10.

The scaled SOCs are compared with $v_1 + v_2$ and $v_1 - v_2$ as shown in Fig. 9(d). The correlation coefficients between $v_1 + v_2$, $v_1 - v_2$ and SOC_1, SOC_2 are 0.9951 and 0.9834, respectively. The result confirms that the slow-time state variable is embedded (or reconstructed) in the smoothest SOCs as indicated by topological similarity of phase portraits in Fig. 10.

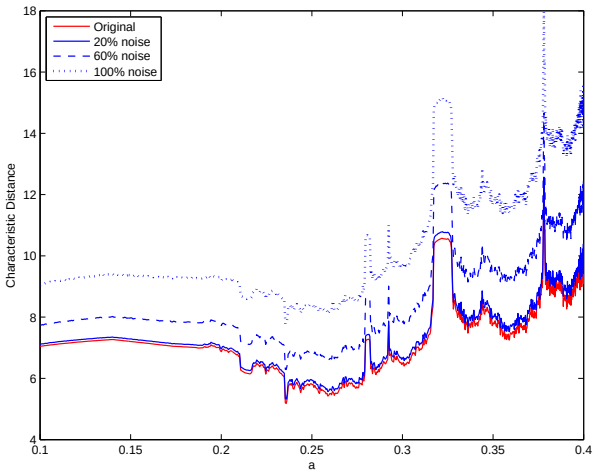

Fig. 11: Characteristic distances of one fixed point.

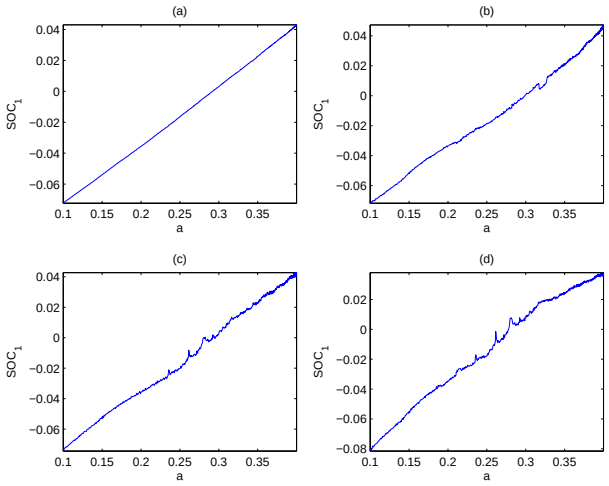

Fig. 12: Tracking results. (a) no noise; (b) 20% noise; (c) 60% noise; (d) 100% noise.

6 Noise Effects

To illustrate the robustness of characteristic distances to noise, normally distributed random noise was added to Rössler's attractor at 1/5, 3/5 and 5/5 RMS amplitude ratios, which corresponds to 20%, 60% and 100% noise in the signal. Fig. 11 shows that the characteristic distances for a particular fixed point drift under the presence of noise. However, the shape of the plot of characteristic distance versus bifurcation parameter a does not change noticeably. The tracking results of slow state variable are shown in Fig. 12. Even for 100% noise, our method still recovers the real slow state variable.

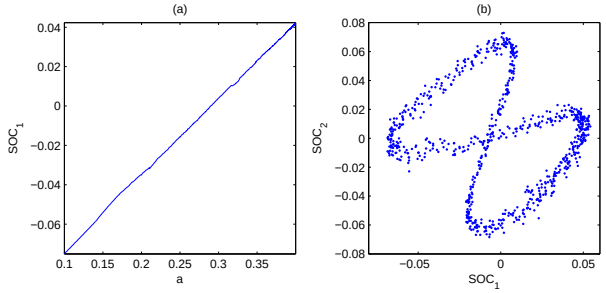

Fig. 13: (a). Tracking a parameter in Rössler equation; (b). Phase portrait of two smoothest SOCs in the experimental data.

7 Discussion

The application of the SOD was warranted by the assumption that feature vectors were in smooth functional relationship with the slow-time state variables. In our simulation examples, the systems exhibited complicated bifurcations while one of the parameters was varied slowly. Therefore, individually, the estimated characteristic distances were not smooth function of the drifting parameters. However, when we combined the characteristic distances from different fixed points and applied SOD to the tracking matrix, we recovered the corresponding smooth deterministic trends, which can be used for one-to-one tracking even in noisy environments.

We also studied the quality of tracking results versus the number of fixed points and their locations. In numerical simulation, 50 fixed points were sufficient. However, in the experiment, we need 300 feature vectors to obtain robust results. To reduce the required number of fixed points and complexity of the tracking matrix, instead of using characteristic distances, we also used characteristic positions as defined in Eq. (5). For example, in the Rössler simulation, instead of using 50 fixed points, we used characteristic positions of only 20 points for tracking (see Fig. 13(a) for the tracking result). For experimental data, characteristic positions of 60 points are enough to obtain reliable result in comparison with characteristic distances of 300 points as shown in Fig. 13(b).

8 Conclusion

Birkhoff Ergodic theorem for measure preserving transformation was used to develop a new class of nonlinear metrics for dynamical systems. In particular, a characteristic distance metric was defined by the average distance from a fixed point in a phase space to all points on the attractor, and the characteristic position was given by the normalized average location of the attractor with respect to a fixed point. These metrics were shown to be sensitive to small parameter changes in a system, and were used to track and identify these changes in conjunction with smooth orthogonal decomposition. The main advantage of these metrics was that they were simple and easy to calculate, while also being robust to noise. These properties make them suitable for online, real-time applications. Numerical simulations, synthetic data, and experiments were used to show how the slowly evolving parameters can be continuously tracked and identified using the considered metrics.

References

1. Abarbanel, H.: Analysis of observed chaotic data. Institute for nonlinear science. Springer (1996)
2. B.Dingwell, J.: Lyapunov Exponents. John Wiley and Sons, Inc. (2006)
3. Chelidze, D., Cusumano, J.P.: Phase space warping: Nonlinear time series analysis for slowly drifting systems. Philosophical Transactions of the Royal Society A **364** (2006)
4. Chelidze, D., Cusumano, J.P., Chatterjee, A.: Dynamical Systems Approach to Damage Evalution Tracking, Part I: Desccription and Experimental Application. Journal of Vibration and Acoustics **124**(2), 250–257 (2002)
5. Chelidze, D., Liu, M.: Dynamical systems approach to fatigue damage identification. Journal of Sound and Vibration **281**, 887–904 (2004)
6. Chelidze, D., Liu, M.: Multidimensional damage identification based on phase space warping: An experimental study. Nonlinear Dynamics **46**(1–2), 887–904 (2006)
7. Clement, A., Laurens, S.: An alternative to the Lyapunov exponent as a damage sensitive feature. Smart Materials and Structures **20**(2) (2011)
8. Cusumano, J., Kimble, B.: A stochastic interrogation method for experimental measurements of global dynamics and basin evolution: Application to a two-well oscillator. Nonlinear Dynamics **8**(2), 213–235 (1995)
9. Donner, R.V., Barbosa, S.M. (eds.): Nonlinear Time Series Analysis in the Geosciences - Applications in Climatology, Geodynamics and Solar-Terrestrial Physics. Berlin: Springer (2008)
10. EtehadTavakol, M., Ng, E.Y.K., Lucas, C., Sadri, S., Ataei, M.: Nonlinear analysis using Lyapunov exponents in breast thermograms to identify abnormal lesions. Infrared Physics & Technology **55**(4), 345 – 352 (2012)
11. Ghafari, S., Golnaraghi, F., Ismail, F.: Effect of localized faults on chaotic vibration of rolling element bearings. Nonlinear Dynamics **53**, 287–301 (2008)
12. Hosseinifard, B., Moradi, M.H., Rostami, R.: Classifying depression patients and normal subjects using machine learning techniques and nonlinear features from {EEG} signal. Computer Methods and Programs in Biomedicine **109**(3), 339 – 345 (2013)
13. Kacimi, S., Laurens, S.: The correlation dimension: A robust chaotic feature for classifying acoustic emission signals generated in construction materials. Journal of Applied Physics **106**(2), 024909 (2009)

14. Kantz, H., Schreiber, T.: Nonlinear Time Series Analysis. Cambridge University Press (2004)
15. Moon, F., Holmes, P.J.: A magnetoelastic strange attractor. Journal of Sound and Vibration **65**(2), 275–296 (1979)
16. Nichols, J., Todd, M.: Nonlinear Features for SHM Applications. John Wiley & Sons, Ltd (2009)
17. Todd, M.D., Nichols, J.M., Pecora, L.M., Virgin, L.N.: Vibration-based damage assessment utilizing state space geometry changes: local attractor variance ratio. Smart Materials and Structures **10**(5), 1000–1008 (2001)
18. Wang, W., Chen, J., Wu, X., Wu, Z.: The application of some non-linear methods in rotating machinery fault diagnosis. Mechanical Systems and Signal Processing **15**(4), 697 – 705 (2001)
19. Wang, W.J., Wu, Z.T., Chen, J.: Fault identification in rotating machinery using the correlation dimension and bispectra. Nonlinear Dynamics **25**(4), 383–393 (2001)
20. Wolf, A.: Quantifying chaos with Lyapuonov exponents, pp. 273–290. Princeton University Press (1986)
21. Yuri, M.P.: Dynamical Systems and Ergodic Theory. Cambridge University Press (1998)